Science AAAS

Solid-State Qubits with Current-Controlled Coupling

T. Hime, *et al.*
Science **314**, 1427 (2006);
DOI: 10.1126/science.1134388

3. G. V. Bicknell, M. C. Begelman, *Astrophys. J.* **467**, 597 (1996).
4. P. L. Biermann *et al.*, *Nucl. Phys. B Proc. Suppl.* **87**, 417 (2000).
5. R. J. Protheroe *et al.*, *Astropart. Phys.* **19**, 559 (2003).
6. F. Aharonian *et al.*, HEGRA collaboration, *Astron. Astrophys.* **403**, L1 (2003).
7. S. Le Bohec *et al.*, *Astrophys. J.* **610**, 156 (2004).
8. W. Hofmann, *Proc. 29th Int. Cosmic Ray Conf. (Pune)*, **10**, 97 (2005).
9. F. Aharonian *et al.*, H.E.S.S. collaboration, *Astropart. Phys.* **22**, 109 (2004).
10. W. Benbow, *Proceedings: Towards a Network of Atmospheric Cherenkov Detectors VII (Palaiseau)*, 163 (2005).
11. M. de Naurois, *Proceedings: Towards a Network of Atmospheric Cherenkov Detectors VII (Palaiseau)*, 149 (2005); http://arxiv.org/abs/astro-ph/0607247.
12. Materials and methods are available as supporting online material on *Science* Online.
13. C. Ma *et al.*, *Astronom. J.* **116**, 516 (1998).
14. M. Beilicke *et al.*, *Proc. of TEXAS Symposium on Relativistic Astrophysics* (Stanford University), Paper #2403 (2004), see http://arxiv.org/abs/astro-ph/0504395.
15. C. Pfrommer, T. A. Enßlin, *Astron. Astrophys.* **407**, L73 (2003).
16. Emission from a region that is moving with a relativistic speed $\beta = v/c$ (c is the speed of light) is boosted along the direction of movement (relativistic beaming). The boost is a function of the observation angle θ relative to this direction and is described by the Doppler factor $\delta = [\Gamma(1-\beta\cos\theta)]^{-1}$, where $\Gamma = (1-\beta^2)^{-1/2}$ is the Lorentz factor of the emission region.
17. E. A. Baltz *et al.*, *Phys. Rev. D* **61**, 3514 (2000).
18. L. Stawarz *et al.*, *Astrophys. J.* **626**, 120 (2005).
19. E. S. Perlman, A. S. Wilson, *Astrophys. J.* **627**, 140 (2005).
20. D. E. Harris *et al.*, *Astrophys. J.* **640**, 211 (2006).
21. D. E. Harris *et al.*, *Astrophys. J.* **586**, L41 (2003).
22. L. Stawarz *et al.*, *Mon. Not. R. Astron. Soc.* **370**, 981 (2006).
23. W. Forman *et al.*, *Astrophys. J.* **635**, 894 (2005).
24. M. Georganopoulos *et al.*, *Astrophys. J.* **634**, L33 (2005).
25. A. Reimer *et al.*, *Astron. Astrophys.* **419**, 89 (2004).
26. D. L. Band, J. E. Grindlay, *Astrophys. J.* **308**, 576 (1986).
27. W. Junor, J. A. Biretta, M. Livio, *Nature* **401**, 891 (1999).
28. C. S. Reynolds, T. di Matteo, A. C. Fabian, U. Hwang, C. R. Canizares, *Mon. Not. R. Astron. Soc.* **283**, L111 (1996).
29. A. Levinson, *Phys. Rev. Lett.* **85**, 912 (2000).
30. E. Boldt, M. Loewenstein, *Mon. Not. R. Astron. Soc.* **316**, 29 (2000).
31. F. A. Aharonian, A. A. Belyanin, E. V. Derishev, V. V. Kocharovsky, Vl. V. Kocharovsky, *Phys. Rev. D* **66**, 023005 (2002).
32. F. N. Owen *et al.*, *Proceedings of The Universe at Low Radio Frequencies, ASP Conf. Ser.*, 199 (2000); http://xxx.lanl.gov/abs/astro-ph/0006152.
33. Provided by D. Harris, private communication.

34. The support of the Namibian authorities and of the University of Namibia in facilitating the construction and operation of H.E.S.S. is gratefully acknowledged, as is the support by the German Ministry for Education and Research (BMBF), the Max Planck Society, the French Ministry for Research, the CNRS-IN2P3, and the Astroparticle Interdisciplinary Programme of the CNRS, the UK Particle Physics and Astronomy Research Council (PPARC), the Institute of Particle and Nuclear Physics of the Charles University, the South African Department of Science and Technology and National Research Foundation, and the University of Namibia. We thank D. Harris for providing the Chandra x-ray light curve of the M87 nucleus.

Supporting Online Material

www.sciencemag.org/cgi/content/full/1134408/DC1
Materials and Methods
SOM Text
Figs. S1 and S2
Table S1
References

28 August 2006; accepted 11 October 2006
Published online 26 October 2006;
10.1126/science.1134408
Include this information when citing this paper.

Solid-State Qubits with Current-Controlled Coupling

T. Hime,[1] P. A. Reichardt,[1] B. L. T. Plourde,[1,2] T. L. Robertson,[1]* C.-E. Wu,[1]† A. V. Ustinov,[1]‡ John Clarke[1]§

The ability to switch the coupling between quantum bits (qubits) on and off is essential for implementing many quantum-computing algorithms. We demonstrated such control with two flux qubits coupled together through their mutual inductances and through the dc superconducting quantum interference device (SQUID) that reads out their magnetic flux states. A bias current applied to the SQUID in the zero-voltage state induced a change in the dynamic inductance, reducing the coupling energy controllably to zero and reversing its sign.

The past few years have seen major advances in the field of superconducting quantum bits (qubits). This family includes those based on electrical charge (*1*), magnetic flux (*2*–*4*), charge and phase (*5*), and the phase difference across a Josephson junction (*6*). Arbitrary superpositions of the single-qubit states can be prepared and manipulated by microwaves to produce Rabi oscillations, Ramsey fringes, and echoes long-familiar in atomic physics and nuclear magnetic resonance (*7*). The prepared quantum states remain coherent for times up to several microseconds (*8*). Coupling two or more qubits together results in entangled states (*9*–*15*) with energy spectra that exhibit the avoided crossings (anticrossings) predicted by quantum mechanics (*16*). In addition to studying quantum coherence in many-body systems, there is considerable interest in arrays of qubits for quantum computing. Because quantum computation requires both the manipulation of single qubits and the entanglement of many qubits, the ability to switch the coupling (*17*–*21*) between qubits on and off in a scalable architecture would enable many quantum-computing algorithms.

[1]Department of Physics, University of California, Berkeley, CA 94720–7300, USA. [2]Department of Physics, Syracuse University, Syracuse, NY 13244–1130, USA.

*Present address: Proteus Biomedical, 750 Chesapeake Drive, Redwood City, CA 94063, USA.

†Present address: Department of Physics, National Tsing-hua University, Hsinchu 300, Taiwan.

‡Permanent address: Physikalisches Institut III, Universität Erlangen-Nürnberg, Erwin-Rommel-Strasse 1, D-91058 Erlangen, Germany.

§To whom correspondence should be addressed. E-mail: jclarke@berkeley.edu

We conducted experiments on two flux qubits biased at the same frequency. In this regime, the antiferromagnetic interaction between the qubits produces an anticrossing and thus a splitting in the energy spectrum of the first and second excited states. By varying the bias current in the zero-voltage state of the superconducting quantum interference device (SQUID) used to read out the flux states of the coupled qubits, we reduced the coupling energy and hence the splitting of the two energy levels of the excited states to zero. Indeed, as predicted, we can even change the interaction from antiferromagnetic to ferromagnetic. Furthermore, we showed that the transition probability from the symmetric ground state to an antisymmetric excited state vanishes at the anticrossing, in qualitative agreement with calculations.

Each flux qubit consists of a superconducting loop interrupted by three Josephson tunnel junctions (*2*). When the applied magnetic flux Φ_q is at the degeneracy point $(n + ½)\Phi_0$ (where n is an integer such that $|\Phi_q - n\Phi_0| \leq \Phi_0/2$, $\Phi_0 \equiv h/2e$ is the flux quantum, h is the Planck constant, and e is the electron charge), a screening current I_q can flow around the loop in either direction, represented by the states $|\uparrow\rangle$ and $|\downarrow\rangle$. The ground and first excited states of the qubit correspond to symmetric and antisymmetric superpositions of the two current states and are separated by an energy Δ. When $\Phi_q \neq (n + ½)\Phi_0$, the energy difference increases to $\nu = (\Delta^2 + \varepsilon^2)^{½}$, where $\varepsilon = 2I_q[\Phi_q - (n + ½)\Phi_0]$. The state of the qubit is measured by coupling the flux generated by I_q to a dc SQUID. Two flux qubits are coupled through their mutual inductances to each other and to the SQUID. The interaction of two pairs of states produces four new states: a ground state $|0\rangle$ and three excited states $|1\rangle$, $|2\rangle$, and $|3\rangle$. Each of these states consists of a linear superposition of four basis states (*22*): the symmetric triplet $|\uparrow\uparrow\rangle$, $|S\rangle = (|\uparrow\downarrow\rangle + |\downarrow\uparrow\rangle)/2^{½}$, and $|\downarrow\downarrow\rangle$ and the antisymmetric singlet $|A\rangle = (|\uparrow\downarrow\rangle - |\downarrow\uparrow\rangle)/2^{½}$.

The two qubits A and B and their readout dc SQUID are shown schematically in Fig. 1A. The qubits have loop inductances L_{qA} and L_{qB} and are coupled through a mutual inductance M_{qq}. The surrounding dc SQUID consists of a loop with inductance L_S and two Josephson junctions, each with critical current I_0. The SQUID is coupled to qubits A and B through mutual inductances M_{qAS} and M_{qBS}. We can pass a bias current I_b through the SQUID and bias the qubits with independent applied fluxes Φ_A and Φ_B; these determine the applied SQUID flux Φ_S. By varying the bias current through the SQUID in the zero-voltage state, we showed theoretically that one can control the coupling energy K between the two qubits (*19*). The energy $K = K_0 + K_S$ has two contributions: a fixed energy K_0 through the mutual inductance of the two qubits, and a controllable energy K_S through their mutual inductances to the SQUID. In the zero-voltage state of a SQUID with appropriate parameters, the inverse dynamic inductance $\mathcal{L}^{-1} = \mathrm{Re}(\partial J/\partial\Phi_S)_{I_b}$ is nonlinear and can be positive, negative, or zero, depending on the values of Φ_S and I_b; Re indicates the real part, and J is the current circulating in the SQUID loop. As a result, the sign of the flux change coupled to (for example) qubit B through the SQUID by a given flux change in qubit A can be chosen to be positive, negative, or zero. The coupling energy K takes the form (*19*)

$$K = K_0 + K_S = 2I_{qA}I_{qB} \times (-M_{qq} - M_{qAS}\,M_{qBS}/\mathcal{L}) \quad (1)$$

where I_{qA} and I_{qB} are the qubit screening currents.

Figure 1B shows our experimental realization of the two qubits and their common SQUID. Our qubits have much larger areas than the three-junction qubits that have been described by other groups (*3*, *12*), and consequently we must take into account their geometrical inductances in simulating their characteristics (*23*). These large areas, together with the on-chip flux lines, enable us to apply independent flux biases using modest currents (~0.3 mA/Φ_0). We deliberately gave the two qubits slightly different areas and mutual inductances to the SQUID so that we could distinguish their flux signals. We measured the SQUID critical current by applying current pulses (Fig. 1C). For each measurement, using 10^5 current pulses, we adjusted the height of the first plateau to obtain a 50% probability of switching out of the zero-voltage state. We applied a pulse of microwave flux to the qubits before each current pulse to drive transitions between quantum states of the individual or coupled qubits, producing peaks and dips in the SQUID switching probability; we plotted the microwave frequency versus the applied flux to obtain energy spectra.

In Fig. 2A, we show the joint frequency spectrum of the qubits. The two flux lines enable us to keep the total flux applied to the SQUID nearly constant by applying fluxes of opposite sign to the qubits (*24*). Each spectrum arises from transitions from the ground state to the first excited state. Except near their apparent intersection, the spectra are excellent fits (dashed lines) to the prediction $\nu = (\Delta^2 + \varepsilon^2)^{1/2}$, yielding $\Delta_A/h = 8.872 \pm 0.005$ GHz and $\Delta_B/h = 8.990 \pm 0.004$ GHz (where errors are SD). An expanded view of the spectra near their intersection at 11.25 GHz (Fig. 2B) reveals an avoided crossing. The lower and upper spectra correspond to transitions from the ground state |0> to the first excited state |1> and the second excited state |2>, respectively. We fitted a hyperbolic curve to each data set to find a splitting of 122.6 ± 0.8 MHz.

The peaks in the lower spectrum of Fig. 2B vanish near the anticrossing, implying that the matrix elements vanish for transitions from |0> to |1>. The origin of this effect lies in the symmetry of the eigenstates (fig. S1). For $K < 0$, the contribution of the antisymmetric singlet state at the anticrossing vanishes for |0>, |2>, and |3>, leaving only contributions from the symmetric triplet states, whereas the converse is true for the state |1>. Consequently, transitions from the symmetric ground state |0> to the antisymmetric excited state |1> are forbidden.

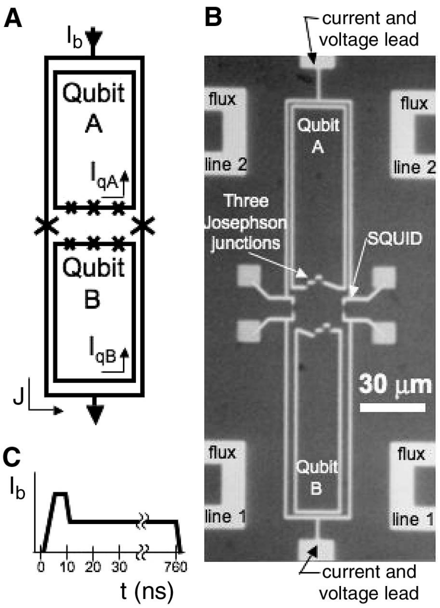

Fig. 1. Coupled flux qubits. (**A**) Two qubits, A and B, surrounded by the dc SQUID used to measure their magnetic flux states and control their inductive coupling. (**B**) The SQUID and the two qubits are fabricated on a Si chip from Al thin films in the same process, using two-angle evaporation; an intervening oxidation process forms the Josephson junctions. The SQUID junctions are 215 × 250 nm^2 and the qubit junctions are 180 × 205 nm^2 (two larger junctions) and 150 × 170 nm^2 (smaller junction). Film widths are 1 μm. Flux lines 1 and 2, connected (separately) in series, apply independent magnetic fluxes to the qubits and SQUID. The chip is enclosed in a superconducting box, and cooled to 50 mK in a dilution refrigerator. (**C**) Current pulse I_b used to determine the critical current.

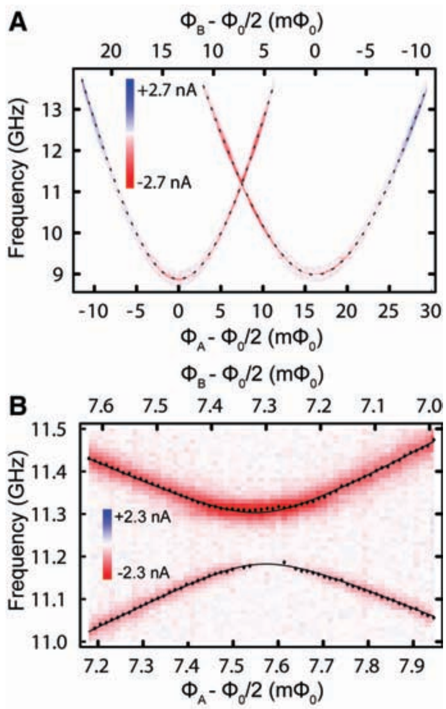

Fig. 2. Frequency versus flux for qubits. (**A**) Spectra of qubits A and B with their fluxes adjusted independently to separate their degeneracy points while keeping the flux applied to the SQUID nearly constant. Data were acquired in a 400-MHz bandwidth around the calculated peak centers. On this scale, the spectra appear to intersect at 11.25 GHz. Color bar indicates peak heights. (**B**) Spectrum shown in (A) expanded to reveal the anticrossing of the spectra of |1> and |2> of the coupled qubits; dots indicate the positions of maximum peak heights. Lower and upper spectra correspond to transitions from the ground state |0> to the excited states |1> and |2>, respectively. Frequency splitting at the anticrossing is 122.6 ± 0.8 MHz. Note the absence of data for |1> near the anticrossing.

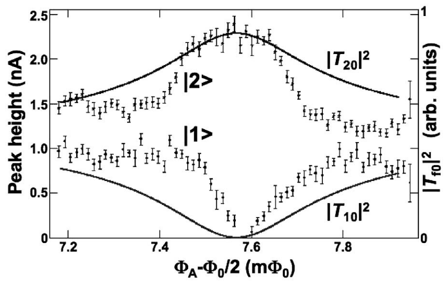

Fig. 3. Measured peak heights and calculated transition probabilities for transitions from the initial state |0> to the final states |1> and |2>. Flux dependence of measured peak heights taken from the spectra in Fig. 2B and of calculated square of matrix elements $|T_{10}|^2$ and $|T_{20}|^2$. $|T_{20}|^2$ is fitted to the peaks at the maximum peak height [measured in arbitrary (arb.) units].

This behavior is illustrated in Fig. 3, where we plot the measured peak heights taken from Fig. 2B. For the transitions from $|0\rangle$ to $|1\rangle$, the amplitude of the peaks becomes vanishingly small at the anticrossing, whereas the peaks are enhanced for the transitions from $|0\rangle$ to $|2\rangle$. Because the peak heights represent the probability of a transition for each measurement, we expected them to scale as the square of the matrix element $T_{f0} = \langle f|\sigma_z^{(A)} + \sigma_z^{(B)}|0\rangle$, where $f = 1,2$ is the final state and $\sigma_z^{(A)}$ and $\sigma_z^{(B)}$ are the Pauli spin operators, characterizing the coupling of the microwave excitation to the qubits. Figure 3 also shows the dependence of $|T_{10}|^2$ and $|T_{20}|^2$ on flux. There is a clear qualitative agreement between the peak heights and the transition probabilities.

In Fig. 4, A to C, at the slightly lower frequency of 10.75 GHz, we show our ability to control the coupling by applying a bias current to the SQUID. The bias current was switched on before the microwave pulse was applied (Fig. 4D, inset); this prebias current I_{pb} was low enough to ensure that the probability of the SQUID switching out of the zero-voltage state would be negligible. Within 10 ns of the microwaves being switched off, we increased the bias current to provide the readout pulse. We fitted hyperbolas to the data and corrected for the flux shift generated by the bias current in the SQUID during the measurement process [supporting online material (SOM) text]. We show our central result in Fig. 4D, where we plot the splitting versus I_{pb} for two different intersection frequencies. For both data sets, the splitting decreases smoothly as I_{pb} is increased. In the case of the data obtained at 10.75 GHz, the splitting goes almost to zero as I_{pb} is increased, and then increases. We believe that this result implies that the coupling was reduced to zero and subsequently changed sign as I_{pb} was increased. Higher values of I_{pb} caused the SQUID to switch prematurely. The two solid curves are the results of our simulations that used only the measured and calculated parameters listed in the caption to Fig. 4D. The calculated curves overestimate the splitting at zero bias current by about 28% and at the prebias current by about 15%. Given the many parameters in the theory and the uncertainties in some of them, we feel that the agreement with experiment is remarkably good. The dashed curves show fits to the data using common values of SQUID critical current and prebias current. The fits are excellent.

The ability to measure the quantum states of two qubits and to switch their coupling on and off with a single SQUID solely by means of its bias current represents an efficient architecture for a quantum computer. In particular, we have shown previously (*19*) that a quantum controlled-NOT logic gate can be implemented with this principle and would provide all the necessary ingredients to implement scalable universal quantum logic. Independent flux lines for the qubits are key to this scalable architecture; it is worth emphasizing, however, that these fluxes remain constant, and one needs only to switch a small current (~ 1 μA) in the SQUID to turn the interaction on and off.

Note added in proof: S. H. W. van der Ploeg *et al.* (preprint available at http://arxiv.org/abs/cond-mat/0605588) reported two flux qubits in which the coupling was controlled by means of a coupler loop and demonstrated that the sign of the ground state could be changed from antiferromagnetic to ferromagnetic. Spectroscopy of excited states was not described.

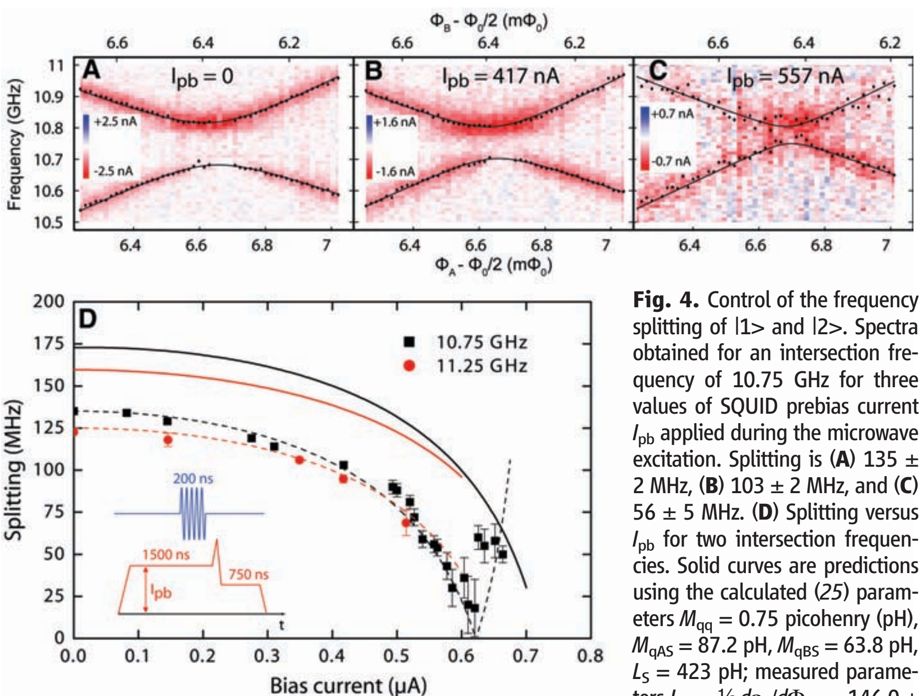

Fig. 4. Control of the frequency splitting of |1> and |2>. Spectra obtained for an intersection frequency of 10.75 GHz for three values of SQUID prebias current I_{pb} applied during the microwave excitation. Splitting is (**A**) 135 ± 2 MHz, (**B**) 103 ± 2 MHz, and (**C**) 56 ± 5 MHz. (**D**) Splitting versus I_{pb} for two intersection frequencies. Solid curves are predictions using the calculated (*25*) parameters $M_{qq} = 0.75$ picohenry (pH), $M_{qAS} = 87.2$ pH, $M_{qBS} = 63.8$ pH, $L_S = 423$ pH; measured parameters $I_{qA} = \frac{1}{2} d\varepsilon_A/d\Phi_{qA} = 146.0 \pm 0.2$ nA, $I_{qB} = \frac{1}{2} d\varepsilon_B/d\Phi_{qB} = 147.8 \pm 0.2$ nA, $\Phi_S(11.25\text{ GHz}) = 0.27\ \Phi_0$, $\Phi_S(10.75\text{ GHz}) = 0.28\ \Phi_0$; and the estimated maximum SQUID critical current $2I_0 = \pi\Delta_s/2eR_{NN} = 1.21 \pm 0.054$ μA, where $\Delta_s = 175 \pm 5$ μeV is the energy gap of Al, and $R_{NN} = 228 \pm 10$ ohms is the resistance of the SQUID at voltages much greater than Δ_s/e. Uncertainties in the low-temperature impedances prevent precise determination of the currents, and we fitted the data using $2I_0 = 0.844$ μA and scaling the bias current by a factor of 0.767. Inset shows pulse sequence.

References and Notes

1. Y. Nakamura, Y. A. Pashkin, J. S. Tsai, *Nature* **398**, 786 (1999).
2. J. E. Mooij *et al.*, *Science* **285**, 1036 (1999).
3. C. H. van der Wal *et al.*, *Science* **290**, 773 (2000).
4. J. R. Friedman, V. Patel, W. Chen, S. K. Tolpygo, J. E. Lukens, *Nature* **406**, 43 (2000).
5. D. Vion *et al.*, *Science* **296**, 886 (2002).
6. J. M. Martinis, S. Nam, J. Aumentado, C. Urbina, *Phys. Rev. Lett.* **89**, 117901 (2002).
7. A. Abragam, *The Principles of Nuclear Magnetism* (Clarendon Press, Oxford, 1961).
8. P. Bertet *et al.*, *Phys. Rev. Lett.* **95**, 257002 (2005).
9. A. J. Berkley *et al.*, *Science* **300**, 1548 (2003).
10. T. Yamamoto, Yu. A. Pashkin, O. Astafiev, Y. Nakamura, J. S. Tsai, *Nature* **425**, 941 (2003).
11. Yu. A. Pashkin *et al.*, *Nature* **421**, 823 (2003).
12. A. Izmalkov *et al.*, *Phys. Rev. Lett.* **93**, 037003 (2004).
13. R. McDermott *et al.*, *Science* **307**, 1299 (2005).
14. J. B. Majer, F. G. Paauw, A. C. J. ter Haar, C. J. P. M. Harmans, J. E. Mooij, *Phys. Rev. Lett.* **94**, 090501 (2005).
15. M. Grajcar *et al.*, *Phys. Rev. Lett.* **96**, 047006 (2006).
16. J. Von Neumann, E. Wigner, *Z. Phys.* **30**, 467 (1929).
17. J. Q. You, J. S. Tsai, F. Nori, *Phys. Rev. Lett.* **89**, 197902 (2002).
18. D. V. Averin, C. Bruder, *Phys. Rev. Lett.* **91**, 057003 (2003).
19. B. L. T. Plourde *et al.*, *Phys. Rev. B* **70**, 140501(R) (2004).
20. P. Bertet, C. J. P. M. Harmans, J. E. Mooij, *Phys. Rev. B* **73**, 064512 (2006).
21. A. O. Niskanen, Y. Nakamura, J. S. Tsai, *Phys. Rev. B* **73**, 094506 (2006).
22. M. J. Storcz, F. K. Wilhelm, *Phys. Rev. A.* **67**, 042319 (2003).
23. T. L. Robertson *et al.*, *Phys. Rev. B* **73**, 174526 (2006).
24. B. L. T. Plourde *et al.*, *Phys. Rev. B* **72**, 060506(R) (2005).
25. M. Kamon, M. J. Tsuk, J. K. White, *IEEE Trans. Microw. Theory Tech.* **42**, 1750 (1994).

26. We thank F. Wilhelm for helpful discussions and I. Siddiqi for thoughtful comments on the manuscript. This work was supported by the NSF under grant EIA-020-5641, Air Force Office of Scientific Research under grant F49-620-02-1-0295, Army Research Office under grant DAAD-19-02-1-0187, Advanced Research and Development Activity, and Bavaria California Technology Center.

Supporting Online Material

www.sciencemag.org/cgi/content/full/314/5804/1427/DC1
SOM Text
Fig. S1

28 August 2006; accepted 18 October 2006
10.1126/science.1134388